SCIENCE CHINA
Chemistry

• ARTICLES •

June 2010 Vol.53 No.6: 1337–1345
doi: 10.1007/s11426-010-3188-8

Preparation, characterization, and catalytic performance of a novel methyl-rich Ti-HMS mesoporous molecular sieve with high hydrophobicity

LI XueFeng[1*], XU ZhiHong[1], GAO HuanXin[2] & CHEN QingLing[2]

[1]*College of Chemistry and Chemical Engineering, Xuchang University, Xuchang 461000, China*
[2]*Shanghai Research Institute of Petrochemical Technology, Shanghai 201208, China*

Received July 25, 2009; accepted December 18, 2009

A novel methyl-rich Ti-containing hexagonal mesoporous silica (Ti-HMS) molecular sieve with high hydrophobicity has been prepared by a two-step method involving co-condensation followed by vapor-phase methyl grafting. The sample was characterized by XRD, N_2 adsorption, FTIR, UV-visible and ^{29}Si NMR spectroscopies, TG, ICP-AES, and hydrophilicity measurements, and its catalytic performance was evaluated using the epoxidation of cyclohexene as a probe reaction. The Ti-HMS material retains a typical mesoporous structure and compared with a co-condensed Ti-HMS prepared in a one-step method possesses more methyl groups and higher hydrophobicity, and also exhibits better catalytic activity and selectivity.

two-step methyl grafting, high hydrophobicity, methyl-rich, Ti-HMS, epoxidation of cyclohexene

1 Introduction

The discovery of mesoporous molecular sieves marked a significant milestone in the development of materials science [1–3]. Mesoporous molecular sieves have been widely applied in catalysis, adsorption, and photoelectric devices due to their characteristics such as large and adjustable pores, high thermostability, and easy modification [4]. Mesoporous molecular sieves containing transition metal ions have been shown to possess excellent catalytic activity in oxidation [4], hydrogenation [5], and desulfurization [6] reactions. Mesoporous sieves containing titanium have been mainly used in hydroxylation of aromatic rings and epoxidation of olefins [4]. Previous studies have demonstrated that the epoxidation activity is associated with the dispersity of active sites (tetracoordinated Ti) and the surface hydrophobicity of the molecular sieve [7, 8]. In general, the surface hydrophobicity of catalysts can be improved by hydroxyl condensation at high temperature [9] and grafting with organic groups [10]. The grafting methods include *in situ* condensation-grafting [10, 11] and post synthesis grafting [7, 10, 12, 13]. The former method is accomplished by adding an alkoxysilane (e.g. methyltrimethoxysilane) to the synthesis mixture [10, 11]. The alkoxysilane will hydrolyze and condense with the silicate ester precursor, and thus the organic groups of the alkoxysilane will be introduced into the surface of the pores of the product resulting in the enhancement of the surface hydrophobicity [10, 11]. However, samples prepared by co-condensation have lower crystallinity and weaker framework stability, because the template surfactant can be only eliminated by solvent extraction and cannot be removed by calcination at high temperature [10]. The latter method, the so called "grafting" method, involves organic groups being grafted through condensation of surface Si–OH and alkoxy groups by post-synthesis silylation [7, 12, 13]. Vapor-phase grafting methods are preferable since no solvent is needed, a wide range of easily controlled

*Corresponding author (email: snow_mount@163.com)

temperatures can be employed, and the operating procedures are convenient [7]. However, only the surfaces of the pore entrances can be modified during grafting treatment, and the internal surfaces cannot be easily modified [10]. The disadvantages of both methods would be overcome if condensation could be combined with grafting, but despite its considerable potential significance, such a novel two-step method has not been reported to date.

In this work, a methyl-rich Ti-containing hexagonal mesoporous silica (HMS) molecular sieve was prepared by such a two-step method for the first time. A methyl-containing Ti-HMS was first synthesized by co-condensation through the introduction of methyltrimethoxysilane to the raw gel, and then trimethylsilyl groups were vapor-grafted onto the Ti-HMS. The sample was characterized by a series of techniques and its catalytic activity was evaluated using the epoxidation of cyclohexene as a probe reaction.

2 Experimental

2.1 Direct synthesis of Ti-Me-HMS by co-condensation [2, 11, 14]

Solution A was prepared by mixing 63 g of distilled water and 32.2 g of ethanol, followed by addition of 7.23 g of hexadecylamine (HDA). The mixture was stirred and heated at 50 °C to facilitate dissolution of HDA. Solution B was prepared by adding a moles of methyltrimethoxysilane (MTMOS) and 0.68 g of tetrabutyltitanate (TBOT) to a mixture of 6 g of isopropanol and b moles of tetraethoxysilane (TEOS) with vigorous stirring for 30 min. Solution B was slowly poured into solution A, followed by stirring for 18 h, filtration, washing, and drying at 110 °C for 24 h. Finally, the as-synthesized sample was refluxed for 1 h in ethanol containing a small amount of ammonium chloride, and then filtered, and washed. The refluxing treatment was carried out 6 times. The sample was dried at 110 °C for 24 h, and then calcined at 300 °C for 8 h. Samples are designated as Ti-Me-HMS-x, where $x = 0$, 0.1, 0.2, and 0.3, is the value of a(MTMOS)/(a(MTMOS) + b(TEOS)) or the molar ratio of MTMOS in the silicon source.

2.2 Vapor-phase methyl grafting of Ti-Me-HMS [7, 9, 13, 15]

The vapor-phase grafting process was carried out in a 2 cm quartz tube reactor, with the sample bed being heated using a tube furnace with a temperature programmed device. 2 g of a sample of Ti-Me-HMS was put into the quartz tube and pretreated at 300 °C for 2 h in a nitrogen flow, and then grafted with a mixture of nitrogen and hexamethyldisilazane (HMDS). Finally, a flow of nitrogen was passed over the sample for 2 h to remove the unreacted HMDS. The resulting samples are designated as 3Me-Ti-Me-HMS-x.

The preparation process is summarized in Scheme 1.

2.3 Characterization

X-ray powder diffraction (XRD) was performed on a Philips (the Netherlands) X'Pert MPD diffractometer using Cu K_α radiation with $\lambda = 0.15418$ nm, tube voltage of 40 kV, tube current of 30 mA, and scanning speed of 2°/min in the 2θ angle range 1°–8°.

N_2-adsorption measurements at low temperature were performed on an automatic ASAP 2010 instrument from Micrometrics (USA). Samples were pretreated at 200 °C for 3 h before adsorption. The specific surface area of samples was calculated based on the BET formula. The pore volume and diameter were calculated based on the BJH method.

Scanning electron microscope (SEM) and transmission electron microscope (TEM) observations were made using Philips XL 30 and JEOL JEM-2010 microscopes, respectively.

Fourier transform infra-red (FTIR) spectra were recorded using a Bruker (USA) IFS88 spectrometer and the samples were analyzed as KBr wafers.

^{29}Si nuclear magnetic resonance spectra with cross-polarization and magic-angle spinning (^{29}Si CP/MAS NMR) were collected on a Bruker (USA) MSL-400 WB spectrometer and ^{29}Si chemical shifts are given with respect to tetramethylsilane.

Thermogravimetric analysis (TGA) was carried out on a DuPont instrument using an alumina crucible. The test

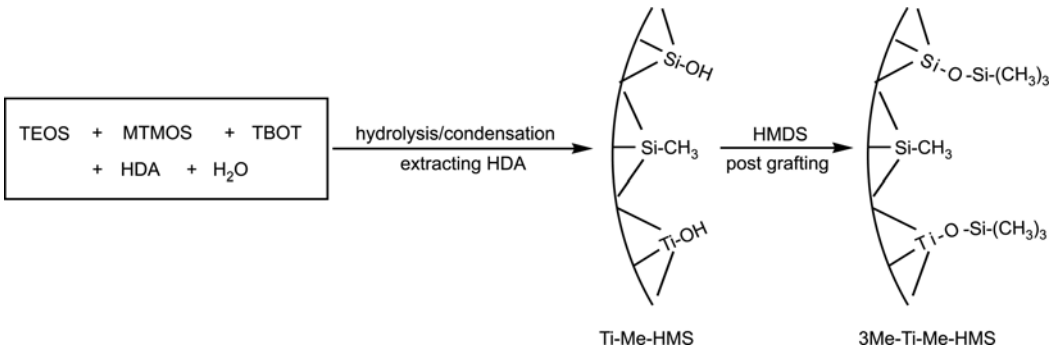

Scheme 1 Schematic illustration of the procedure for preparing a methyl-rich Ti-HMS with high hydrophobicity by the two-step method.

temperature ranged from room temperature to 1000 °C. The differential curve of the TG trace is designated as DTG.

The Ti content was determined by inductively coupled plasma-atomic emission spectrometry (ICP–AES) using a Thermo Jarrell Ash IRIS Advantage 1000 instrument.

Diffuse reflectance ultraviolet–visible spectroscopy (DR UV–visible) spectra were recorded on a Perkin Elmer 555 double beam spectrophotometer with $BaSO_4$ as reference and slit width of 2.0 nm. The samples were fast scanned.

Hydrophilicity tests were carried out as follows: A weighed bottle containing the sample was put in a thermostat containing saturated NaCl solution and weighed again after adsorbing water for 72 h. The hydrophilicity was calculated using the following equation:

$$H = 100\% \times \left(m_a - m_b\right)/m_b$$

where m_a and m_b stand for the sample weight after and before adsorbing water, respectively.

2.4 Evaluation of catalytic performance

The catalytic performance of the materials was evaluated in the epoxidation of cyclohexene (CH) using cumene hydroperoxide (CHP) as oxidant. All reactions were carried out in a 100 mL glass reactor. In a typical procedure, 0.3 g of catalyst were transferred to a reaction mixture of 33% (*w*/*w*) CH, 53% CHP, 11.5% cumene, and 2.5% *n*-octane (as internal standard), and the mixture was allowed to react at 70 °C for 2 h. The CHP consumption was determined by standard iodometric titration. The reaction products were analyzed using an HP4890 gas chromatograph equipped with a capillary column (HP-1) and a flame ionization detector (FID). Analysis showed that the reaction products consisted of a mixture of cyclohexene oxide (CHO), cyclohexanediol (CHD), cyclohexanone, and α-hydroxylcyclohexene. However, the contents of cyclohexanone and α-hydroxylcyclohexene accounted for only ~1% of the total products, and therefore only CHO and CHD are considered as the products of epoxidation. The conversion of CHP (X_{CHP}), efficiency of CHP (E_{CHP}), and the selectivity to CHO (S_{CHO}) are defined as the following equations:

$$X_{CHP} = 100\%\left(\left[CHP\right]_0 - \left[CHP\right]\right)/\left[CHP\right]_0$$

$$E_{CHP} = 100\% \times \left(\left[CHO\right] + \left[CHD\right]\right)/\left(\left[CHP\right]_0 - \left[CHP\right]\right)$$

$$S_{CHO} = 100\% \times \left[CHO\right]/\left(\left[CHO\right] + \left[CHD\right]\right)$$

where $[CHP]_0$ and [CHP] stand for the initial and final concentrations of CHP (mol/L), respectively, and [CHO] and [CHD] stand for the final concentrations of CHO and CHD (mol/L), respectively.

3 Results and discussion

3.1 XRD

The XRD patterns of the samples (Figure 1) all show a main peak at low angle (2θ= ca. 2°) assigned to the (100) reflection, and no other diffraction peaks are seen at higher angles. This indicates that all the samples have long range order but do not have any short range order; this is characteristic of HMS mesoporous materials [2, 14]. The intensity of the (100) peak decreases with increasing amount of MTMOS because of the reduction of sample crystallinity associated with the introduction of methylsilyl groups into the HMS framework. The 2θ angle increases with the increase in amount of MTMOS indicating a decrease in the unit cell parameters. The intensity of the 100 peak increases significantly after vapor-phase grafting, suggesting that this is accompanied by an enhancement of the local regularity of the crystal surface.

3.2 N_2 adsorption measurements

The N_2 adsorption isotherms and pore diameter distributions are displayed in Figures 2 and 3. All the Ti-Me-HMS-*x*

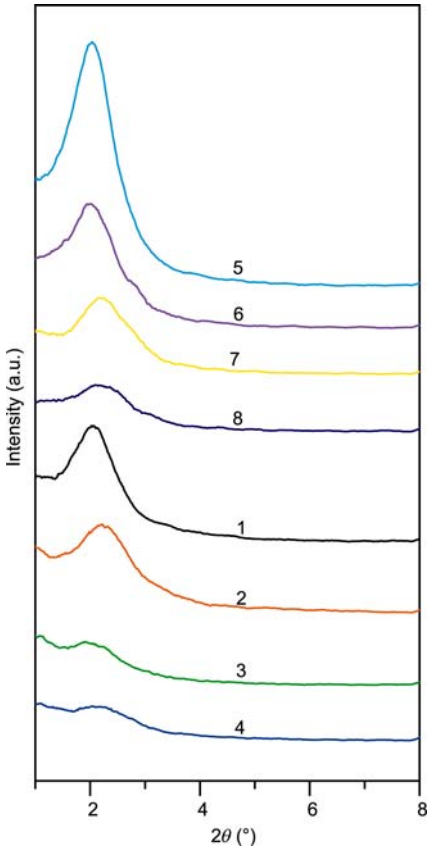

Figure 1 XRD patterns of samples. 1, Ti-Me-HMS-0; 2, Ti-Me-HMS-0.1; 3, Ti-Me-HMS-0.2; 4, Ti-Me-HMS-0.3; 5, 3Me-Ti-Me-HMS-0; 6, 3Me-Ti-Me-HMS-0.1; 7, 3Me-Ti-Me-HMS-0.2; 8, 3Me-Ti-Me-HMS-0.3.

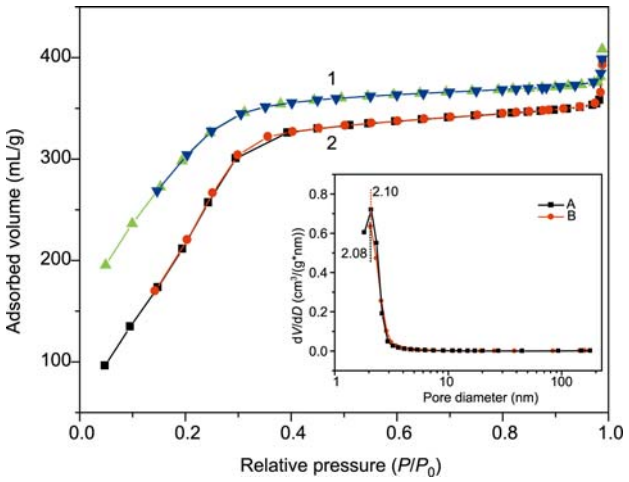

Figure 2 N_2-adsorption isotherms and pore size distributions of Ti-Me-HMS-0.1 (1) and 3Me-Ti-Me-HMS-0.1 (2).

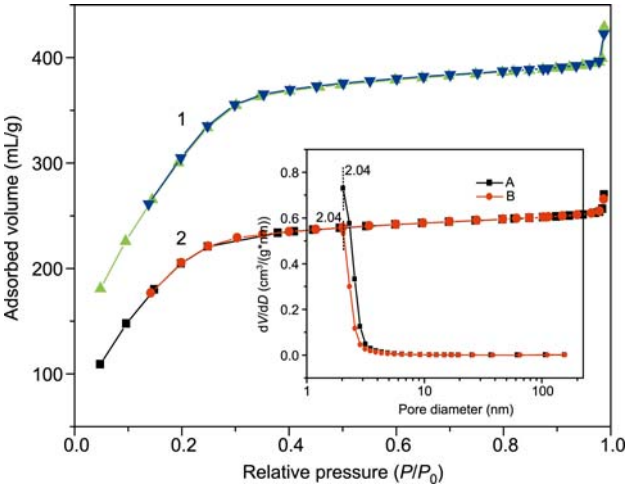

Figure 3 N_2-adsorption isotherms and pore size distributions of Ti-Me-HMS-0.3 (1) and 3Me-Ti-Me-HMS-0.3 (2).

samples show type IV isotherms and most probable pore diameters of about 2 nm, both typical characteristics of mesoporous materials [2]. The lower relative pressure (P/P_0) regions of the isotherms indicate that the samples possess a number of micropores, and therefore have high specific surface areas (see Table 1). This is likely to be due to new porosity resulting from condensation of methylhydroxylsilyl groups formed as products of methyltrimethoxysilane hydrolysis and the lower shrinkage level among pore walls resulting from calcination at low temperatures [11].

As shown in Figures 2 and 3, the typical IV isotherms of samples are retained after post-condensation vapor-phase grafting, while the most probable pore diameter is slightly reduced and the adsorbed volume is greatly reduced because grafting of trimethylsilyl groups on the surface of Ti-Me-HMS leads to a decrease in pore diameter [7]. Furthermore, the decrease in the adsorbed volume after grafting is less for Ti-Me-HMS-0.1 than for Ti-Me-HMS-0.3, which may be due to the more efficient introduction of methyl groups into Ti-Me-HMS-0.3 by direct synthesis (co-condensation) [7]. Moreover, the sharp rises in the isotherms of the grafted samples at high relative pressure (P/P_0 = ca. 0.99) resulting from the capillary condensation occur at lower relative pressures after grafting, indicating the grafting of trimethylsilyl groups on the external surface of Ti-Me-HMS mesoporous materials leads to a decrease in pore diameter [7].

3.3 SEM and TEM

SEM images of Ti-Me-HMS-0.3 and 3Me-Ti-Me-HMS-0.3 are displayed in Figure 4. The uniform microparticles in directly synthesized Ti-Me-HMS-0.3, as well as the grain size and uniformity, are all almost unchanged after post-condensation vapor-phase grafting, suggesting that the morphologies of the materials are not significantly affected by the grafting process.

The TEM images in Figure 5 show that the mesoporous structure of the sample is retained after grafting because the "worm-like" pore structure of Ti-Me-HMS-0.3 is essentially unchanged [2].

3.4 FTIR spectroscopy

FTIR spectra of Ti-Me-HMS samples are shown in Figure 6.

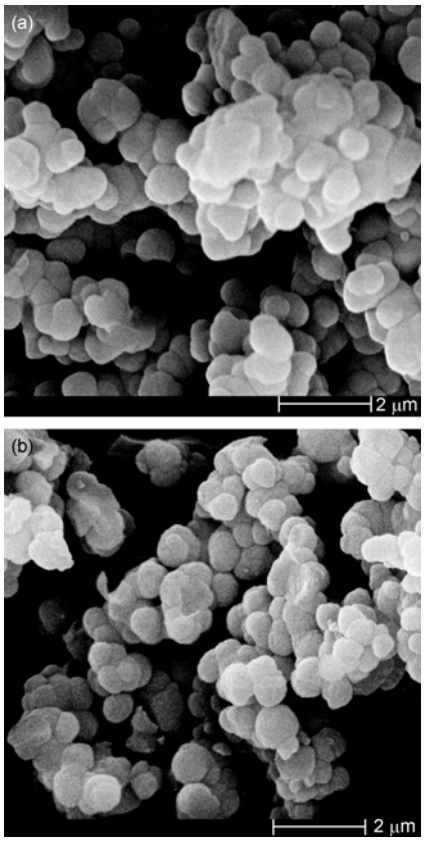

Figure 4 SEM images of Ti-Me-HMS-0.3 (a) and 3Me-Ti-Me-HMS-0.3 (b).

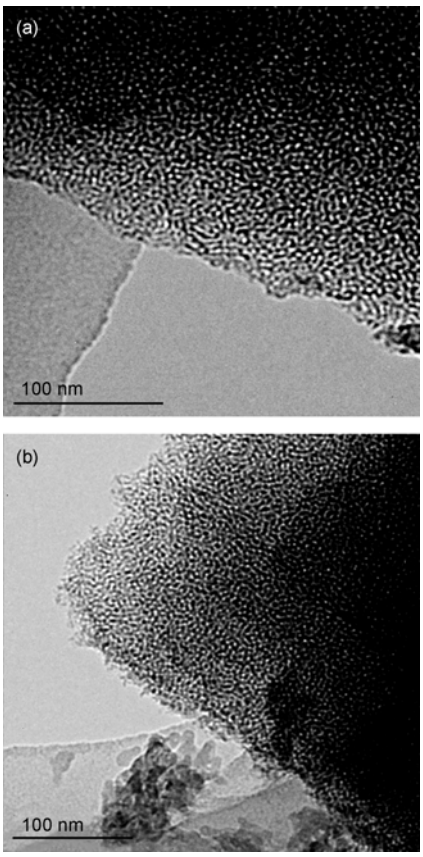

Figure 5 TEM images of Ti-Me-HMS-0.3 (a) and 3Me-Ti-Me-HMS-0.3 (b).

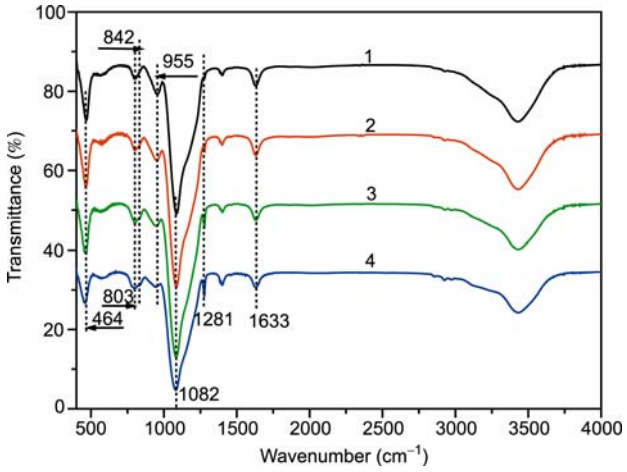

Figure 6 FTIR spectra of Ti-Me-HMS-0 (1), Ti-Me-HMS-0.1 (2), Ti-Me-HMS-0.2 (3) and Ti-Me-HMS-0.3 (4).

Bands are assigned to adsorbed water on hydrogen-bonded silanol groups located at 3300–3700 cm^{-1}, C–H stretching of grafted methyl groups [15] at 2976, 2932 and 1413 cm^{-1}, water adsorbed on silanol groups at 1633 cm^{-1}, Si–CH_3 stretching [12] at 1281 cm^{-1}, Si–O–Si antisymmetric stretching at 1082 cm^{-1}, S–O and Si–O–Ti vibrations [16, 17] at 950–960 cm^{-1}, C–H bending vibrations [13] at 842 cm^{-1}, Si–O–Si framework symmetric stretching vibrations at 803 cm^{-1}, and silanol bending [18] at 464 cm^{-1}.

As the methyl content of the materials is increased from Ti-Me-HMS-0 to Ti-Me-HMS-3 the intensities of bands at 3738, 3300–3700, 1630, 955 and 464 cm^{-1} related to silanol groups all decrease, whilst the intensities of bands at 2976, 2932, 1413, 1462, 1281 and 842 cm^{-1} related to methyl groups all increase. This confirms that methyl groups have been successively introduced into Ti-HMS, and that the hydrophobicity of Ti-Me-HMS increases with increasing methyl content. Moreover, the band at 955 cm^{-1} is intense and sharp for samples with fewer methyl groups, whilst its intensity is decreased and shifted to 945 cm^{-1} with increasing incorporation of methyl groups. This is because that the band at 955 cm^{-1} represents the overlap of the 940 cm^{-1} band of Si–O–Ti and the 969 cm^{-1} band of Si–OH, and the band intensity is decreased as $Si(OSi)_3CH_3$ groups replace $Si(OSi)_3OH$ and the overlapping band is shifted to lower wavenumbers [17].

The spectra of 3Me-Ti-Me-HMS in Figure 7 show that the bands ascribed to methyl groups have been distinctly changed after vapor-phase grafting: the intensities of Si–C stretching bands at 750 cm^{-1}, Si–CH_3 bands at 850 cm^{-1}, and C–H bands at 2932 and 2976 cm^{-1} are all increased, confirming that trimethylsilyl groups have been grafted onto the surface of Ti-Me-HMS [12, 13, 15].

3.5 ^{29}Si CP/MAS NMR spectroscopy

Figure 8 gives the ^{29}Si CP/MAS NMR spectra of Ti-Me-HMS-0, Ti-Me-HMS-0.3 and 3Me-Ti-Me-HMS-0.3. Peaks at −109, −100 and −90 ppm are attributed to Q^4 ($(SiO)_4Si^*$), Q^3 ($(SiO)_3Si^*OH$), and Q^2 ($(SiO)_2Si^*(OH)_2$), respectively [7, 13]. Peaks at −63 and −54 ppm are attributed to $T^3(MeSi^*(OSi)_3)$ and $T^2(Me(OH)Si^*(OSi)_2)$ resulting from

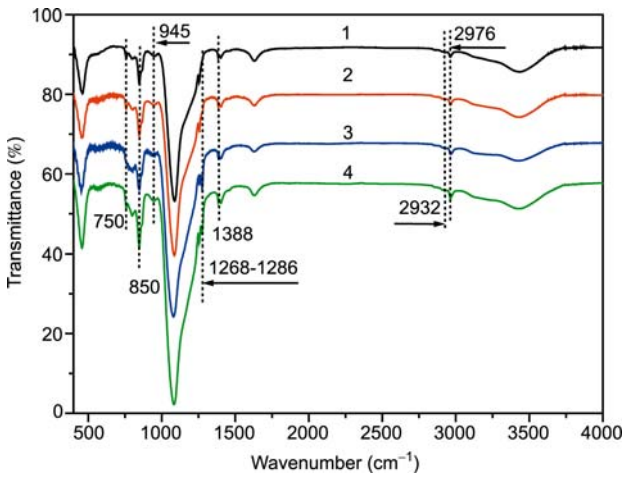

Figure 7 FTIR spectra of 3Me-Ti-Me-HMS-0 (1), 3Me-Ti-Me-HMS-0.1 (2), 3Me-Ti-Me-HMS-0.2 (3) and 3Me-Ti-Me-HMS-0.3 (4).

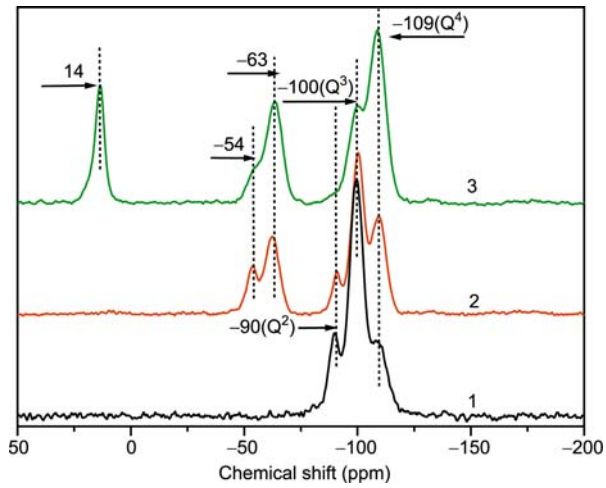

Figure 8 ^{29}Si CP/MAS NMR spectra of Ti-Me-HMS-0 (1), Ti-Me-HMS-0.3 (2) and 3Me-Ti-Me-HMS-0.3 (3).

different degrees of condensation between methylsilyl and silanol groups [11, 16]. As shown in Figure 8, the $Q^4/(Q^2+Q^3+Q^4)$ ratios of Ti-Me-HMS-0.3 and 3Me-Ti-Me-HMS-0.3 are higher than that of Ti-Me-HMS-0, suggesting the Q_4 content increases after methyl grafting. The above results indicate that methyl groups have been grafted onto the framework of Ti-HMS. Ti-Me-HMS contains considerable amounts Q^2 and Q^3 because many lone ($Q^3(SiO)_3Si$*-OH)) and geminal ($Q^2((SiO)_2Si$*-$(OH)_2)$) silanol groups have been retained due to the relatively low calcination temperature (300 °C). The peak at 14 ppm is characteristic of $(CH_3)_3Si$*$O(SiO)_3$ groups formed by linkage of trimethylsilyl and silanol groups after vapor-phase grafting [7, 13]. Furthermore, as shown in Figure 8, the T^3 contents are also greatly increased after vapor-phase grafting of Ti-Me-HMS, suggesting that large numbers of silanol groups have been eliminated.

3.6 TGA (TG–DTG)

Figure 9 shows TG–DTG curves of Ti-Me-HMS-0.3 and 3Me-Ti-Me-HMS-0.3.

The weight loss below 170 °C is ascribed to the removal of physisorbed water, that at 230–400 °C ascribed to loss of chemisorbed water and residual organic template (HDA), that at 400–700 °C ascribed to thermal decomposition and oxidation of methyl groups, and that above 700 °C ascribed to condensation and framework reforming of silanol groups [7, 17].

As shown in Figure 9, the weight loss within the range 400–700 °C in the DTG curve of Ti-Me-HMS-0.3 indicates that methylsilyl groups have been introduced into the molecular sieve framework. Ti-Me-HMS-0.3 has higher weight loss within the temperature range 400–700 °C than Ti-Me-HMS-0.3, showing that both methylsilyl and trimethylsilyl groups have been introduced into the framework [7, 17].

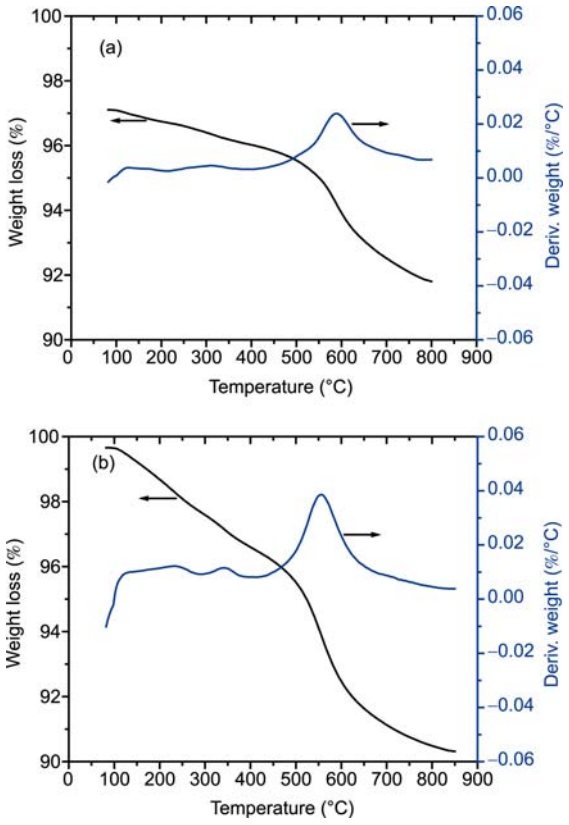

Figure 9 TG-DTG curves of Ti-Me-HMS-0.3 (a) and 3Me-Ti-Me-HMS-0.3 (b).

Figure 10 shows the relationship between weight loss and x value (a(MTMOS)/(a(MTMOS) + b(TEOS))) within the temperature range 400–700 °C for Ti-Me-HMS and 3Me-Ti-Me-HMS samples. The methyl content of Ti-Me-HMS increases with x and their relationship is linear. Meanwhile, the total methyl content decreases with x because samples with lower values of x, e.g. Ti-Me-HMS-0.1 have

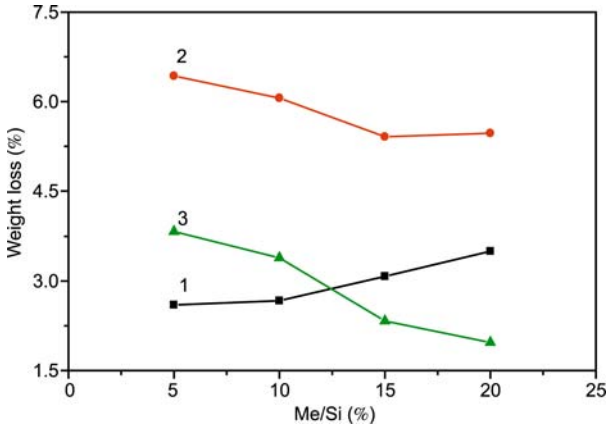

Figure 10 Comparison of weight loss of samples in the temperature range 400–700 °C. 1, The weight loss trend of Ti-Me-HMS; 2, the weight loss trend of 3Me-Ti-Me-HMS; 3, the difference between the weight losses of Ti-Me-HMS and 3Me-Ti-Me-HMS.

more silanol groups to condense with trimethylsilyl groups whereas the samples with larger values of x have fewer silanol groups and more methyl groups, thus decreasing the content of grafted trimethylsilyl groups.

These conclusions are consistent with the decrease in the difference in methyl contents of 3Me-Ti-Me-HMS before and after vapor-phase grafting. The above results show that with increasing MTMOS dosage (increasing value of x), the methyl group contents of Ti-Me-HMS formed by direct synthesis increase whereas the methyl group contents of 3Me-Ti-Me-HMS formed by vapor-phase grafting decrease.

3.7 Hydrophilicity measurements

Table 1 shows that Ti-Me-HMS-x (x = 0.1, 0.2, 0.3) samples have much lower water adsorbing ratios (hydrophilicity) than Ti-Me-HMS-0 without methyl groups, suggesting that the hydrophobicity has been significantly improved by introducing methyl groups. The water adsorbing ratios decrease gradually with increasing MTMOS dosage, suggesting that the hydrophobicity increases with the content of methyl groups. This is consistent with the TGA data. The water adsorbing ratios of 3Me-Ti-Me-HMS are dramatically reduced after vapor-phase grafting, suggesting that the residual silanol groups have been eliminated by grafting of trimethylsilyl groups, which further enhances the surface hydrophobicity.

Figure 11 shows the physical states of Ti-Me-HMS-0.3 and 3Me-Ti-Me-HMS-0.3 in water and visually reflects the difference in hydrophilicity/hydrophobicity before and after vapor-phase grafting. Almost all of 3Me-Ti-Me-HMS-0.3 powder floats on the water surface whereas most of Ti-Me-HMS-0.3 powders sinks down, suggesting that Ti-Me-HMS-0.3 has high hydrophilicity and 3Me-Ti-Me-HMS-0.3 has very low hydrophilicity as a result of vapor-phase grafting.

3.8 ICP–AES

Table 1 shows that Si/Ti ratios in Ti-Me-HMS-x samples decrease with the increasing value of x and increasing methyl group content, suggesting that the Ti content increases with increasing methyl group content. This is consistent with the results reported by Igarashi [11] (for Ti-MCM-41 grafted *in situ* by phenyl groups) and Bhaumik [16] (for Ti-MCM-41 grafted *in situ* by methyl groups). After vapor-phase grafting of trimethylsilyl groups, the Ti content decreases because the Si content increases as trimethylsilyl groups are grafted to the Ti-Me-HMS.

3.9 DR UV–visible spectroscopy

Figures 12 and 13 show the DR UV–visible spectra of Ti-Me-HMS-0.1 and Ti-Me-HMS-0.3 before and after vapor-phase grafting, respectively. Ti-Me-HMS-0.1 and Ti-Me-HMS-0.3 exhibit an intense peak at 217–220 nm ascribed to tetracoordinated Ti species and the peak shifts to 212–215 nm after vapor-phase grafting. A similar blue shift has been attributed by Peña [7] to the opened tetracoordi nated Ti being transformed to an enclosed tetracoordinated Ti species. Moreover, the peak intensity decreases after vapor-phase grafting because of the decrease in Ti content (increase in Si content) [7].

3.10 Catalytic performance

As shown in Table 1, CHP conversion over Ti-Me-HMS-x increases slightly with increasing value of x; this can be attributed to the corresponding increase in Ti content. Both conversion and efficiency of CHP are increased after vapor-phase grafting because the number of acidic –OH sites is reduced after trimethylsilyl groups are grafted onto Si–OH and Ti–OH (the content of opened Ti sites increases) which reduces the decomposition side reactions of CHP. Furthermore, CHO selectivities of 3Me-Ti-Me-HMS-x are near to 100% after vapor-phase grafting because the hydrophilicities of the catalysts have been greatly reduced which prevents ring opening of epoxides. This results in the selectivity of the catalysts being improved and the rate of deactivation being reduced [7, 15]. However, the increases in catalytic

Table 1 Physicochemical properties and catalytic performance of catalysts

Sample number	Si/Ti (mol mol^{-1})	S_{BET} (m^2 g^{-1})	$D^{a)}$ (nm)	$V^{b)}$ (cm^3 g^{-1})	$H^{c)}$ (%)	X_{CHP} (%)	E_{CHP} (%)	S_{CHO} (%)
Ti-Me-HMS-0	79	–[d)]	–	–	19.2	64.3	93.4	97.5
Ti-Me-HMS-0.1	73	1144.5	2.10	0.632	13.5	66.4	93.0	97.6
Ti-Me-HMS-0.2	68	–	–	–	8.1	68.8	92.8	97.0
Ti-Me-HMS-0.3	64	1197.5	2.04	0.664	7.0	70.7	92.6	96.5
3Me-Ti-Me-HMS-0	117	–	–	–	0.08	72.1	99.3	100
3Me-Ti-Me-HMS-0.1	110	1060.2	2.08	0.615	0.13	74.7	98.0	99.8
3Me-Ti-Me-HMS-0.2	103	–	–	–	0.10	77.1	99.5	100
3Me-Ti-Me-HMS-0.3	99	820.3	2.04	0.418	0.10	79.6	98.0	100

a) Average pore diameter; b) pore volume calculated from BET measurements; c) hydrophilicity of samples measured on the basis of the method in Section 2.3; d) –, not measured.

Figure 11 Illustrations of the physical states of 3Me-Ti-Me-HMS-0.3 (1) and Ti-Me-HMS-0.3 (2) in water.

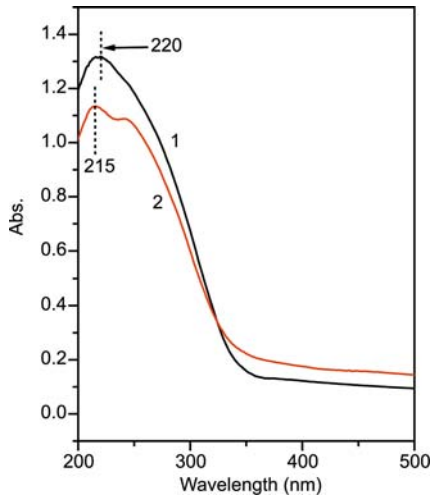

Figure 12 DR UV-visible spectra of Ti-Me-HMS-0.1 (1) and 3Me-Ti-Me-HMS-0.1 (2).

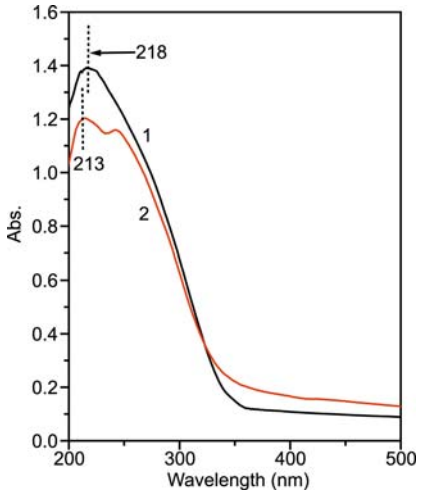

Figure 13 DR UV-visible spectra of Ti-Me-HMS-0.3 (1) and 3Me-Ti-Me-HMS-0.3 (2).

activity (CHP conversion) over 3Me-Ti-Me-HMS-*x* are slight after vapor-phase grafting because the Ti contents of Ti-Me-HMS before grafting are low. Therefore, future work must focus on how to enhance the Ti contents in molecular sieve samples prepared by the co-condensation method.

4 Conclusions

The highly hydrophobic 3Me-Ti-Me-HMS mesoporous molecular sieve catalyst was prepared by co-condensation of TEOS and MTMOS, in order to introduce methyl groups in the product (Ti-Me-HMS), followed by grafting of trimethylsilyl groups for surface modification.

The characterization results show that Ti-Me-HMS has a typical mesoporous structure and high surface hydrophobicity. The grafting process results in the pore diameter and specific surface area of 3Me-Ti-Me-HMS being reduced to some extent compared with Ti-Me-HMS, whilst the mesoporous structure is retained and the hydrophobicity is significantly enhanced.

The activity and selectivity of 3Me-Ti-Me-HMS in the epoxidation of cyclohexene are higher than Ti-Me-HMS, showing the beneficial effect of the vapor-phase grafting process. On vapor-phase grafting, the content of acidic Ti–OH and Si–OH sites is significantly reduced, and therefore the surface hydrophobicity of the catalyst is enhanced significantly. As a result, there is a decrease in the amount of decomposition side reactions of CHP and ring opening of epoxides is avoided, and thus the deactivation process is dramatically suppressed .

The above results suggest that further research on the improvement of the two-step method should focus on the following three aspects. Firstly, the solvent extraction process should be improved so that the template can be removed as completely as possible whilst reducing the loss of Ti. The thermal treatment should also be improved in order to increase the condensation degree of surface silanol groups and the molecular sieve framework, which will increase the regularity of the mesopores. Finally, the two-step method should be used to introduce other organic groups such as sulfhydryl, halogen, amino, and epoxy, by means of which the other novel materials will be obtained.

This work was supported by the Key Program for Science and Technology Development of Henan Province (092102210221) and the Program for Natural Science Research of the Education Department of Henan Province (2009B150025).

1 Kresge CT, Leonowicz ME, Roth WJ, Vartuli JC, Beck JS. Ordered mesoporous molecular sieves synthesized by a liquid-crystal template mechanism. *Nature*, 1992, 359: 710–712
2 Tanev PT, Chibwe M, Pinnavaia TJ. Titanium-containing mesoporous molecular sieves for catalytic oxidation of aromatic compounds. *Nature*, 1994, 368: 321–323
3 Zhao DY, Feng JL, Huo QS, Melosh N, Fredrickson GH, Chmelka BF, Stucky GD. Triblock copolymer syntheses of mesoporous silica with periodic 50 to 300 angstrom pores. *Science*, 1998, 279: 548–552
4 Corma A. From microporous to mesoporous molecular sieve materi-

als and their use in catalysis. *Chem Rev*, 1997, 97: 2373–2420
5 Wang YJ, Wang XL, Xie GQ, Lu JQ, Jin WY, Liu XJ, Luo MF. Crotonaldehyde hydrogenation over CuO/SBA-15 catalyst (in Chinese). *J Catal*, 2008, 29: 482–488
6 Hou DM, Zhou F, Li X, Wang LY, Wang AJ. Hydrodesulfurization performance of MCM-41 supported Pd catalysts (in Chinese). *Acta Petrolei Sinica (Petroleum Processing Section)*, 2009, 25: 167–172
7 Peña ML, Dellarocca V, Rey F, Corma A, Coluccia S, Marchese L. Elucidating the local environment of Ti(IV) active sites in Ti-MCM-48: A comparison between silylated and calcined catalysts. *Micropor Mesopor Mater*, 2001, 44–45: 345–356
8 Marchese L, Maschmeyer, T, Gianotti E, Coluccia S, Thomas JM. Probing the titanium sites in Ti-MCM-41 by diffuse reflectance and photoluminescence UV-vis spectroscopies. *J Phys Chem*, 1997, 101: 8836–8838
9 Li KT, Lin PH, Lin SW. Preparation of Ti/SiO_2 catalysts by chemical vapor deposition method for olefin epoxidation with cumene hydroperoxide. *Appl Catal*, 2006, 301: 59–65
10 Melero JA, Grieken R van, Morales G. Advances in the synthesis and catalytic applications of organosulfonic-functionalized mesostructured materials. *Chem Rev*, 2006, 106: 3790–3812
11 Igarashi N, Kidani S, Ahemaito R, Hazuhito H, Tatsumi T. Direct organic functionalization of Ti–MCM-41: Synthesis condition, organic content, and catalytic active. *Micropor Mesopor Mater*, 2005, 81: 97–105
12 Cagnoli MV, Casuscelli SG, Alvarez AM, Bengoa JF, Gallegos NG, Crivello M E, Herrero ER, Marchetti SG. Ti-MCM-41 silylation: Development of a simple methodology for its estimation—Silylation effect on the activity and selectivity in the limonene oxidation with H_2O_2. *Catal Today*, 2005, 107–108: 397–403
13 Lin KF, Wang LF, Meng FY, Sun ZH, Yang Q, Cui YM, Jiang DZ, Xiao FS. Formation of better catalytically active titanium species in Ti-MCM- 41 by vapor-phase silylation. *J Catal*, 2005, 235: 423–427
14 Tuel A. Modification of mesoporous silicas by incorporation of heteroelements in the framework. *Micropor Mesopor Mater*, 1999, 27: 23–33
15 Sever R R, Alcala R, Dumesic J A, Root T W. Vapor-phase silylation of MCM-41 and Ti-MCM-41. *Micropor Mesopor Mater*, 2003, 66: 53–67
16 Bhaumik A, Tatsumi T. Organically modified titanium-rich Ti-MCM-41, efficient catalysts for epoxidation reactions. *J Catal*, 2000, 189: 31–39
17 Müller CA, Maciejewski M, Mallat T, Baiker A. Organically modified titania-silica aerogels for the epoxidation of olefins and allylic alcohols. *J Catal*, 1999, 184: 280–293
18 Zhang MY, Wang LF, Huang ZT. Synthesis conditions and catalytic performance of hexagonal mesoporous silica containing copper (in Chinese). *J Catal*, 2003, 24: 914–918